PENSOFT

SENCKENBERG
NATURE RESEARCH

Leibniz Association

Drivers of Andean diversity: Phylogeographic structure and the evolution of hemipenial and dewlap morphology in a Neotropical lizard (Squamata: Anolidae: *Anolis mariarum*)

Freddy A. Grisales-Martínez[1,2], Juan M. Daza[1]

1 *Grupo Herpetológico de Antioquia GHA, Instituto de Biología, Facultad de Ciencias Exactas y Naturales, Universidad de Antioquia UdeA, Calle 70 No. 52-21, Medellín, Colombia*

2 *Servicios Ambientales y Geográficos S.A. (SAG S.A.), Calle 11B No. 40A-130, Medellín, Colombia*

https://zoobank.org/83D2A69D-3312-41DC-9A7F-9E4FB56FFC6B

Corresponding authors: Freddy A. Grisales-Martínez (grisso88@gmail.com), Juan M. Daza (jumadaza@gmail.com)

Academic editor Uwe Fritz | **Received** 14 April 2026 | **Accepted** 3 September 2026 | **Published** 6 October 2026

Citation: Grisales-Martínez FA, Daza JM (2026) Drivers of Andean diversity: Phylogeographic structure and the evolution of hemipenial and dewlap morphology in a Neotropical lizard (Squamata: Anolidae: *Anolis mariarum*). Vertebrate Zoology 76: 681–697. https://doi.org/10.3897/vz.76.e195284

Abstract

Phenotypic traits and genetic variation are fundamental for understanding biological diversity and evolutionary processes. In natural populations, phenotypic novelties are generally expected to align with genetic differentiation, establishing phenotype–genotype relationships. This pattern is evident in Neotropical lizards of the genus *Anolis*, where traits such as the dewlap and hemipenes play key roles in species recognition and sexual selection, and are often associated with reproductive isolation, genetic structure, and lineage divergence. However, in *Anolis mariarum*, an Andean species from northern Colombia, previous limited sampling suggested a mismatch between these traits and the mitochondrial DNA (mtDNA) lineages. Here, we analyzed specimens from 41 localities across the species' range, examining hemipenial morphology, dewlap coloration, phylogenetic signal, and genetic structure using three mitochondrial markers. We identified seven mitochondrial clades within *A. mariarum*, with divergence partially shaped by Andean topography and genetic distances comparable to those reported among *Anolis* species and subspecies. Two hemipenial morphologies (types A and B) and three dewlap colour patterns (orange–yellow, orange–pink, reddish) were detected, reflecting notable intraspecific variation. Although both traits showed strong phylogenetic signal, they exhibited weak spatial and genetic structuring, suggesting an early stage of divergence. Because our inferences are based exclusively on mtDNA, these results should be interpreted cautiously and provide only a preliminary framework for investigating the evolutionary processes underlying phenotypic diversification. These results highlight the evolutionary relevance of dewlap and hemipenial traits and emphasize the need for extensive morphological, geographic, and genetic sampling to accurately assess lineage boundaries and uncover patterns and processes leading to enormous diversity in Neotropical fauna.

Keywords

Anoles, genotype, mitochondrial DNA, non-plastic trait, phenotype, phylogenetic signal

Introduction

Examining phenotypic traits and genetic variation provides essential insights into the mechanisms driving biological diversity, revealing evolutionary patterns applicable across species (Gallant and O'Connell 2020; Márquez et al. 2020). Although evolution may occasionally proceed through a saltationist mode, whereby drastic

Copyright *Freddy A. Grisales-Martínez* and *Juan M. Daza*. This is an open access article distributed under the terms of the Creative Commons Attribution License (CC BY 4.0), which permits unrestricted use, distribution, and reproduction in any medium, provided the original author and source are credited.

mutations give rise to markedly distinct phenotypes, the emergence of phenotypic novelty is more broadly expected to result from gradual genetic change, establishing a well-characterized genotype–phenotype relationship (Bateman and DiMichele 2002; Jiménez 2021; Wood et al. 2021). Beyond genetic determinism, environmental influences play an equally pivotal role in shaping phenotypic traits, underscoring the complex interplay among genotype, environment, and phenotype (Orgogozo et al. 2015; Ng et al. 2017; Jiménez 2021). These dynamics are particularly evident when contrasting plastic traits, whose expression is primarily modulated by environmental conditions, with non-plastic traits, in which genetic factors predominate, conferring higher heritability (Fusco and Minelli 2010; Lalejini et al. 2021; Turner and Corander 2021).

Non-plastic traits are generally expected to have high evolutionary significance and to be conserved within genetic groups or lineages due to their high heritability and reduced sensitivity to environmental variation. Therefore, a significant challenge in a microevolutionary context arises from findings that phenotypic variation in traits with evolutionary significance does not always align with lineages identified by molecular markers (Gilman et al. 2019; Jiménez 2021; Prates et al. 2021). This potential mismatch highlights the complexity of the genotype-phenotype relationship and underscores the need for a more comprehensive understanding of evolutionary processes. An ideal model for studying the behavior of putatively non-plastic traits and their correspondence at the genotypic level includes organisms with high population densities, high detectability, and phenotypic traits that are both conspicuous and significant for evolutionary and systematics studies, as are some of the external morphological characters of Neotropical lizards in the genus *Anolis* Daudin, 1802.

Anolis lizards are a diverse clade of vertebrates in which phenotypic traits such as dewlap colour pattern and hemipenial morphology (e.g., size and shape) are expected to be conserved within a species, due to their critical role in species recognition and sexual selection (Nicholson et al. 2007; Losos and Schneider 2009; Klaczko et al. 2015; D'Angiolella et al. 2016). Historically, it has been assumed that both dewlap and hemipenial morphology harbor phylogenetic signal in the anole lineage and are frequently used to define species boundaries (Nicholson et al. 2007; Klaczko et al. 2015). In an evolutionary context, phylogenetic signal refers to the tendency of closely related lineages to resemble each other more than expected by chance because traits are inherited from common ancestors (Losos 2008; Revell et al. 2008). Consequently, evaluating phylogenetic signal in these traits provides a direct test of whether phenotypic variation reflects shared evolutionary history or has evolved repeatedly through convergence, local adaptation, or phenotypic plasticity. During the speciation process, traits exhibiting strong phylogenetic signal are expected to track lineage divergence, whereas weak or absent phylogenetic signal suggests that trait evolution has become decoupled from phylogenetic history (Blomberg et al. 2003).

Consistent with this expectation, variation in dewlap coloration and hemipenial morphology has long been assumed to reflect reproductive isolation, genetic structure, and independently evolving lineages (e.g., Ng and Glor 2011; Glor and Laport 2012; Köhler et al. 2012a, 2012b; Ng et al. 2017). Although both traits contribute to reproductive isolation, they are expected to act at different stages of the speciation process. Dewlap coloration functions primarily as a prezygotic behavioral signal involved in mate recognition and sexual selection, promoting assortative mating among individuals with similar signalling traits (Nicholson et al. 2007; Ng and Glor 2011; Ng et al. 2017). In contrast, hemipenial morphology represents a mechanical component of reproductive isolation, potentially affecting successful copulation and sperm transfer once mating occurs, and is therefore expected to evolve rapidly under sexual selection and mechanical compatibility (Klaczko et al. 2015; D'Angiolella et al. 2016). The differences in hemipenial morphology among closely related species have prompted the use of male genitalia as a crucial evolutionary trait (Köhler et al. 2012a, 2012b; Klaczko et al. 2015). Therefore, testing the phylogenetic signal of both traits in *Anolis mariarum* allows us to determine whether their observed variation is consistent with lineage diversification and species boundaries, or whether it reflects evolutionary processes independent of phylogenetic relationships, such as environmental effects or phenotypic plasticity.

Geographically structured variation in dewlap colour patterns, coupled with different hemipenial morphologies, has been observed in *Anolis* lizards, revealing significant differentiation based on mitochondrial markers (Köhler et al. 2010, 2012a, 2012b; Glor and Laport 2012; Köhler and Vargas 2019). This has led to a deeper understanding of genetic structure and phylogenetic divergence, resulting in the proposal of distinct subspecies and species. Such differentiation is expected, as the mitochondrial genome allows for the reconstruction of evolutionary histories across groups, supporting the development of hypotheses about species relationships and population divergence (Harris et al. 2018; Blair 2023). Given the strong correlation between phenotype and genotype, it is necessary to examine mitochondrial markers that are widely used to assess both inter- and intra-specific divergence, to better understand phenotypic traits with evolutionary significance in *Anolis* lizards, such as the dewlap and hemipenes.

Contrary to the expectations, an apparent case of genotype-phenotype discordance is observed in the Blemished Anole, *Anolis mariarum* Barbour, 1932, a species found in the northern Andes of Colombia (Grisales-Martínez et al. 2017). This species exhibits variation in dewlap coloration, with two distinct bicolored morphotypes: one characterized by an orange anterior region and a yellow posterior region, and the other by an orange anterior region and a pink posterior region (Grisales-Martínez et al. 2017). Likewise, hemipenial morphology is polymorphic, with three morphotypes described: Type 1, possessing long lobes with flounces; Type 2, with short lobes lacking flounces; and Type 3, with short lobes and a dermal ridge

(Melo-Torres et al. 2025). However, given the limited sampling in these previous studies (nine individuals for dewlap coloration and five for hemipenial morphology), it remains unclear whether this variation persists with broader sampling and whether these traits exhibit a phylogenetic structure.

Considering the potential role of dewlap and hemipenial morphology as evolutionary drivers, this study tests two hypotheses to explain reproductive trait variation in the Blemished Anole. The first hypothesis predicts that variation in these traits reflects evolutionary divergence among populations. Under this scenario, individuals sharing the same dewlap colour pattern and hemipenial morphotypes should cluster within the same mitochondrial lineages, exhibit significant phylogenetic signal, and display a geographically structured distribution. Alternatively, the second hypothesis predicts that these traits represent intraspecific polymorphisms that are not associated with mitochondrial evolutionary history. Such a pattern may result from phenotypic plasticity or from other evolutionary processes (e.g., introgression, sexual selection, or incomplete lineage sorting). Under this scenario, phenotypic variation is expected to show little or no association with mitochondrial genetic structure, weak or absent phylogenetic signal, and no consistent spatial pattern.

To evaluate these hypotheses, we characterized variation in dewlap colour pattern and hemipenial morphology throughout the distribution of *Anolis mariarum* and assessed the relationship between phenotype, mitochondrial genetic structure, phylogenetic signal, and geographic distribution. Support for the first hypothesis would indicate that these traits are evolutionarily informative characters, useful for species delimitation and for understanding microevolutionary processes. Conversely, support for the second hypothesis would suggest that the observed polymorphisms are not explained by mitochondrial lineage divergence. Because our inferences are based exclusively on haploid mitochondrial markers, such a result should be interpreted cautiously, as it may also reflect processes acting differently on the nuclear genome, thereby limiting the systematic value of these traits when evaluated solely with mitochondrial data.

Materials and Methods

Population sampling

This study was conducted using specimens from historical collections housed at the Museo de Herpetología Universidad de Antioquia (**MHUA**), and additional field collections were carried out under the research permit Resolution 1461 issued by the **ANLA** (Autoridad Nacional de Licencias Ambientales). The additional collected individuals were euthanized using a 5% lidocaine solution, after which muscle tissue samples (hind limbs) were extracted and preserved in 99% ethanol. The specimens were then fixed in 10% formalin and preserved in 70% ethanol. The geographic sampling included the northern Andes between the Western and Central cordilleras, with specimens from 41 localities. A total of 118 individuals of *Anolis mariarum* were examined, of which 65 were categorized based on hemipenial morphology and 70 were characterized for dewlap colour pattern (Table S1).

Genetic data

Total genomic DNA was extracted from ethanol-preserved tissues using the GeneJET Genomic DNA Purification kit (Thermo Fisher Scientific). Three mitochondrial regions were amplified and sequenced. Several nuclear regions were tested as they have been used in reptile systematics above species level (neurotrophin III **NT3**, dynein axonemal heavy chain III **DNAH3**, and prolactin receptor **PRLR**) but little genetic variation was found (data not shown). This is due to the shallow intraspecific variation within *Anolis mariarum*. Therefore, only mitochondrial regions were used. A partial 16S region was amplified using the primers 16SC-L and 16SD-H (Goebel et al. 1999; Santos et al. 2003), the fragment of NADH dehydrogenase subunit II region (**ND2**) and the tRNAs Trp, Ala, Asn, Cys, and Tyr was amplified using the primers Metf6 and L555 (Macey et al. 1997; Castañeda and de Queiroz 2011), and the partial cytochrome *b* region (**cyt *b***) was amplified using the primers GLUDG-L and MVZ16 (Moritz et al. 1992; Palumbi 1996). The Polymerase Chain Reaction (**PCR**) cycling conditions are provided in Table S2. PCR products were purified and sequenced at the Macrogen facilities in Korea. Chromatographs were reviewed, and sequences were manually edited using Geneious Prime 2023.2.1 (https://www.geneious.com).

Phylogenetic analysis

Phylogenetic inference was conducted using Maximum Likelihood (**ML**) and Bayesian Inference (**BI**) to elucidate relationships among individuals. Each mitochondrial region was aligned using MAFFT version 7 with the G-INS-i algorithm under default parameters (Katoh and Standley 2013). For the ND2 and cyt *b* regions, protein translations were reviewed to ensure correct alignment with respect to reading frames. The assembled genetic matrix (File S1) included individuals of *Anolis mariarum*, as well as *Anolis tolimensis* Werner, 1916 and *Anolis antonii* Boulenger, 1908, which were incorporated as closely related taxa based on the phylogenetic hypothesis proposed by Grisales-Martínez et al. (2017). Additionally, we included other species closely allied to the *Anolis fuscoauratus* group (sensu Williams 1976), following the phylogenetic hypothesis by Poe et al. (2017). *Anolis auratus* Daudin, 1802 was used to root the tree. Because of its morphological similarity and taxonomic confusion with *A. mariarum*, to ensure correct species assignment, samples from the type locality were included for both *A. tolimensis* and *A. antonii*.

We inferred a ML tree using IQ-TREE 3.0.1 (Nguyen et al. 2015). We tested seven partitions (16S and the codon positions for each of the coding regions ND2 and cyt *b*; File S2) and selected the best partitioning scheme using ModelFinder (Kalyaanamoorthy et al. 2017) in IQ-TREE using the –m MFP+MERGE option and the "greedy" algorithm (Lanfear et al. 2012). Node support was estimated from 10000 ultrafast bootstrap pseudoreplicates (Hoang et al. 2018). The BI was conducted in MrBayes v3.2 (Ronquist et al. 2012) using the same partitioning scheme and substitution models selected for the ML analysis. Two independent runs of four Markov Chain Monte Carlo (**MCMC**) each (one cold and three heated; temperature = 0.1) were performed for five million generations, sampling every 1000 generations. Convergence was assessed by monitoring the average standard deviation of split frequencies (< 0.01) and effective sample sizes (**ESS** > 200) in Tracer v1.7 (Rambaut et al. 2018). The first 25% of sampled trees were discarded as burn-in, and a 50% majority-rule consensus tree was used to estimate Bayesian posterior probabilities (**PP**) for each node.

Hemipenial morphology

Hemipenes were extracted and processed following Zaher and Prudente (2003) and D'Angiolella et al. (2016). All prepared hemipenes were obtained from fresh specimens, and to minimize potential variation caused by the eversion process, only fully everted hemipenes were used. The organ was everted manually by exerting pressure on the base of the tail. Then, the tip of a needle was inserted into scales surrounding the base of the organ until the tip of the needle was visible inside the organ to inject colored petroleum jelly. Finally, the organ was extracted, the retractor muscle was cut, and the organ was stored in 70% ethanol. The hemipenes were treated with an alcoholic solution of Alizarin to contrast the ornamentation from the surface and reveal deep calcified structures. Terminology for hemipenial structures followed Köhler et al. (2012b) and D'Angiolella et al. (2016).

Allometric analyses were conducted to assess the relationship between hemipenial morphotypes and body size variation in *Anolis mariarum*, using head width (**HW**) and snout–vent length (**SVL**) as morphological proxies. SVL is widely recognized as a standard estimator of overall body size in lizards, whereas HW reflects cranial dimensions often associated with functional performance and sexual selection (Hernández-Salinas et al. 2014). This approach allows us to determine whether hemipenial morphotypes covary with body size scaling or represent size-independent morphological divergence. Linear models were used to test for differences in allometric relationships between morphotypes, while Wilcoxon rank-sum tests (**W**) were applied to assess differences in the distribution of HW and SVL between morphotypes. Analyses were implemented in R (R Core Team 2025) using the package ggplot2 (Wickham 2016).

Dewlap coloration

Male dewlaps of live individuals were photographed using a Nikon Coolpix B700 digital camera with the same settings and flash application throughout the study. Forceps were employed to fully extend the dewlap for all lizards. Dewlap pattern and coloration were discretely characterized through visual inspection, following the pattern categories described by Nicholson et al. (2007). Colours were defined based on the Color Catalogue for Field Biologists (Köhler 2012), and assignments for each dewlap were independently assessed and verified by two observers.

Additionally, using photographs of 70 individuals, we quantified colour differences among dewlap colour patterns by employing a cost-effective and accessible method recently proposed by Jacobs et al. (2023). This method is comparable to the spectrophotometer approach and can effectively distinguish dewlap variation within the visible light spectrum. The technique includes the ImageJ software (Schneider et al. 2012) and the Measure plugin, which quantifies colour intensity on a scale of 0 to 255 in the red, green, and blue (**RGB**) spectrum. Digital field images were standardized using white references, and RGB values were extracted. We analyzed colour from our photographic data based on discriminant analysis of principal components (**DAPC**; Jombart et al. 2010) of RGB colour space. DAPC applies a principal component analysis (**PCA)** transformation as a preliminary step before discriminant analysis, making it particularly effective for evaluating variability among dewlap colour pattern groups while minimizing variation within each group (Jombart et al. 2010). The analysis was performed in R (R Core Team 2025) using the packages adegenet (Jombart 2008), ggplot2 (Wickham 2016), and dplyr (Wickham et al. 2021).

Trait evolution

Phenotypic traits in *Anolis* lizards, have been shown to exhibit geographically structured variation (Glor and Laport 2012; Köhler et al. 2010, 2012a, 2012b). Therefore, we assessed whether dewlap colour patterns and hemipenial types exhibit spatial autocorrelation. We implemented a Local Indicators of Spatial Association (**LISA**) analysis based on Local Moran's I (Anselin 1995), using the localmoran function from the R package spdep (Bivand et al. 2017; R Core Team 2025). To test for trait associations, we performed contingency analyses using Chi-square (χ^2) tests. Given that both dewlap and hemipenial morphology have previously been shown to exhibit phylogenetic signal within the anole lineage (Nicholson et al. 2007; Klaczko et al. 2015), we further evaluated phylogenetic signal for each trait using the delta statistic (δ), an estimator designed for discrete data (Borges et al. 2019). The analyses were performed in R (R Core Team 2025) using the base package along with ape (Paradis et al. 2004) and ggplot2 (Wickham 2016).

Genetic structure

To evaluate whether genetically structured populations align with variation in key phenotypic traits, individuals were grouped in three ways: according to clades identified through the phylogenetic analyses, dewlap colour patterns, and hemipenial morphology (Files S3–11). For each mitochondrial region unrooted statistical haplotype networks based on the Templeton-Crandall-Singh (**TCS**) algorithm (Clement et al. 2000) were constructed. Additionally, an Analysis of Molecular Variance (**AMOVA**) (Excoffier et al. 1992) was performed to assess molecular variation among individuals with different trait states (dewlap colour patterns and hemipenial morphs), as well as between clades. Both analyses were conducted in POPART v.1.7 (Leigh and Bryant 2015).

To further explore the genetic differentiation among clades, population genetic parameters were estimated using DnaSP v. 5.10 (Librado and Rozas 2009). The fixation index ($\mathbf{\Phi_{ST}}$) (an analogous measure to $\mathbf{F_{ST}}$ but for mitochondrial genetic sequence data; Excoffier et al. 1992), average number of pairwise nucleotide differences ($\mathbf{K_{XY}}$), nucleotide substitution per site ($\mathbf{D_{XY}}$), net nucleotide substitution per site ($\mathbf{D_A}$), genetic differentiation index based on the frequency of haplotypes ($\mathbf{G_{ST}}$), and genetic differentiation index based on haplotype frequency and mutational steps between haplotypes ($\mathbf{N_{ST}}$) were estimated. Additionally, mean uncorrected genetic distances (p-distances) between mitochondrial clades were calculated for each mitochondrial marker (16S, ND2, and cyt *b*) in R (R Core Team 2025) using the packages ape (Paradis et al. 2004) and dplyr (Wickham et al. 2021).

Results

Evolutionary relationships

Sequence alignment resulted in a matrix of 2687 sites: 1075 sites of ND2, 812 of 16S and 800 of cyt *b*. The best partition scheme included four partitions and the inferred evolution models were 16S: HKY+F+I+G4, cyt*b*_pos1: K2P+I, cyt*b*_pos2: HKY+F+I, cyt*b*_pos3+ND2pos1+ND2pos2+ND2pos3: TIM2+F+I+G4. ML and BI analyses produced highly congruent topologies, including both basal and terminal relationships. Several main clades were uncovered, with consistently high PP and UFBoot support values (Figs 1; Files S12–S14). We detected substantial genetic divergence among the Andean species of the *Anolis fuscoauratus* group. *Anolis tolimensis* was recovered as sister to *A. mariarum*, whereas *A. antonii* was nested within a clade composed by Central American species (Files S12–14).

The results suggest phylogenetic structure with seven major clades, generally receiving high PP and UFBoot support (Files S12–14). These clades correspond to different parts of the geographic distribution of *Anolis mariarum* and are named accordingly (Fig. 1). Samples from southeastern Antioquia in the Central Andes (southeastern clade) form the most divergent lineage and are recovered as the sister group to all remaining clades. Samples from the northernmost part of the Central Andes in Antioquia (northern_1 clade) form the sister lineage to the remaining five internal clades. Within this group, samples from the northern Central Andes in Antioquia (northern_2 clade) are recovered as sister to a clade that includes specimens from the southernmost areas of Risaralda and Quindío (southern clade), the eastern region of Antioquia (eastern clade), the northern Western Andes (northwestern clade), and the Central and Western Andes (western clade). The latter two form the most closely related pair of clades.

Hemipenes characterization

Two distinct hemipenial morphologies were observed among the 65 examined specimens from 26 localities (Table S1). We refer to these morphotypes as type A and type B. Type A hemipenes have a well-developed bilobed structure, a deep sulcus spermaticus, prominent sulcal lips, and the asulcate apex strongly calyculate. In contrast, type B hemipenes have smaller lobes, a shallow sulcus spermaticus, less pronounced sulcal lips, and moderate calyculation (Fig. S1). The two morphs were recorded in similar proportions, with 30 individuals exhibiting type A and 35 exhibiting type B.

The allometric analysis of hemipenial morphotypes in Anolis mariarum revealed no strong evidence of differences in body size between morphs. For head width (HW), the linear model indicated that individuals with type B hemipenes tended to have slightly larger heads than those with type A, although this effect showed only a weak trend ($F_{1,23} = 3.89$, $p = 0.06$). The non-parametric Wilcoxon rank-sum test confirmed the absence of significant differences ($W = 49$, $p = 0.121$). For snout–vent length (SVL), no differences were detected between morphs, with both the linear model ($F_{1,23} = 0.0008$, $p = 0.978$) and Wilcoxon test ($W = 72$, $p = 0.764$) showing non-significant results. Violin plots of SVL and HW show broad overlap between type A and type B individuals, with similar medians and interquartile ranges in both variables (Fig. S2). Although a few extreme values are present in each group, these do not produce a consistent shift in central tendency or dispersion. Overall, the substantial overlap in body size and head dimensions supports the absence of marked size differentiation between hemipenial morphotypes.

Dewlap characterization

We identified three dewlap colour patterns (in parenthesis colour following Köhler 2012): (i) bicolored with an orange (spectrum to burnt) front and a yellow (trogon to light orange yellow) back, (ii) bicolored with an orange (spectrum to burnt) front and a pink (rose pink to pinkish white) back, and (iii) unicolored, ranging reddish (burnt

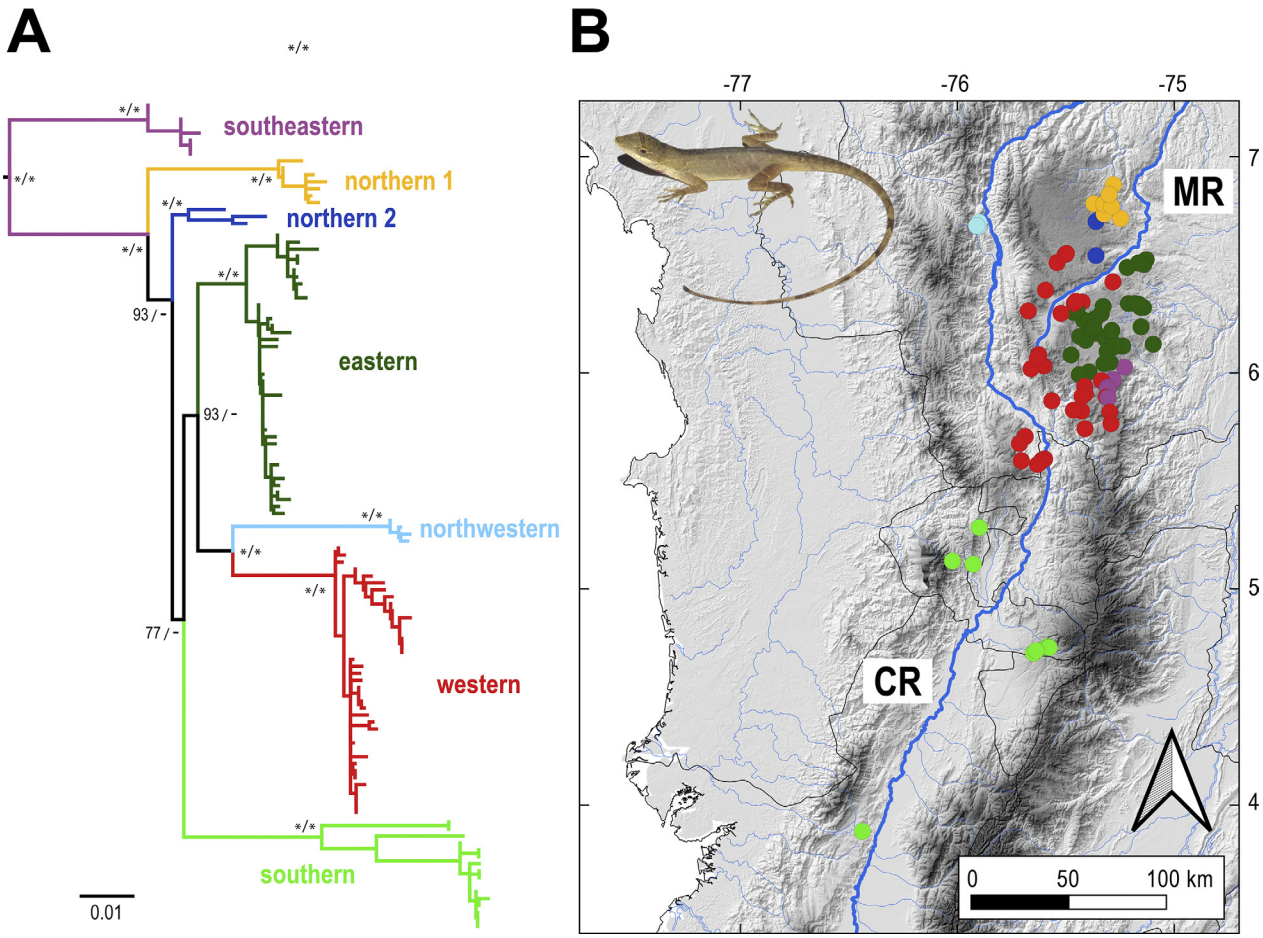

Figure 1. A Maximum likelihood tree (-lnL = –14716.682) depicting evolutionary relationships within the *A. mariarum* inferred from an analysis using 2687 sites, three mtDNA regions (16S, cyt *b*, ND2), and 118 terminals. UFBoot (left/above) and PP (right/below) values are shown. An asterisk (*) indicates UFBoot < 95 and PP < 0.95, whereas a dash (–) indicates UFBoot ≥ 95 and PP ≥ 0.95. Major clades of *A. mariarum* represented in different colours. Each clade is labeled at the front with the same colour. **B** Geographic location the major clades of *A. mariarum*. CR: Cauca River, MR: Medellín River.

orange to peach red) (Fig. S3). In the discriminant analysis of principal components (DAPC) using the populations defined by dewlap colour pattern as a priori groups (orange-pink, orange-yellow, reddish), the first two discriminant functions clearly separate the three categories (Fig. S4). The first two eigenvalues, the horizontal and vertical axes, were large, representing 88% and 11.9% of the variation respectively, indicating that most of the between group variation was captured in the analysis.

Trait evolution

The genetic matrix included 75 adult males of *Anolis mariarum*. Of these, 60 have phenotypic information for both traits, 10 for dewlap colour pattern only, and five for hemipenial morphology. Both traits appear multiple times across the tree and trait combinations are randomly distributed: type A occurs with orange-pink (13), orange-yellow (8), and reddish (5); type B with orange-pink (22), orange-yellow (11), and reddish (1) (Fig. 2). The delta test revealed a significant phylogenetic signal for both traits in *A. mariarum* (Fig. S5). Dewlap colour pattern showed an observed $\delta = 5.38$ ($p < 0.05$). Similarly, hemipenial morphology exhibited a strong signal ($\delta = 7.7$, $p < 0.05$). However, the two traits appear to vary independently: the Chi-square test ($\chi^2 = 4.821$, df = 2, $p = 0.090$) showed no significant association between dewlap colour pattern and hemipenial morphology.

The analysis of dewlap variation in *Anolis mariarum* using Local Moran's I did not reveal strong evidence of overall spatial autocorrelation, with values ranging from –1.68 to 0.49. Approximately 10% of individuals showed significant local associations ($p < 0.05$); however, no local clusters of the same morph were detected. The orange-pink dewlap has a wider distribution, occurring on both sides of the Cauca River Valley in the Central and Western Andes, while the orange-yellow and reddish dewlaps are restricted to the Central Andes on both sides of the Medellín River Valley. However, all three dewlap colour patterns are either found in close proximity or overlap in certain areas (Fig. 3). Similarly, the analysis of hemipenial variation in A. mariarum using Local Moran's I did not reveal strong evidence of overall spatial autocorrelation, with values ranging from –1.0 to 1.13. However, approximately 25% of individuals showed significant local associations ($p < 0.05$), with positive values indicating local clusters of the same morph, particularly

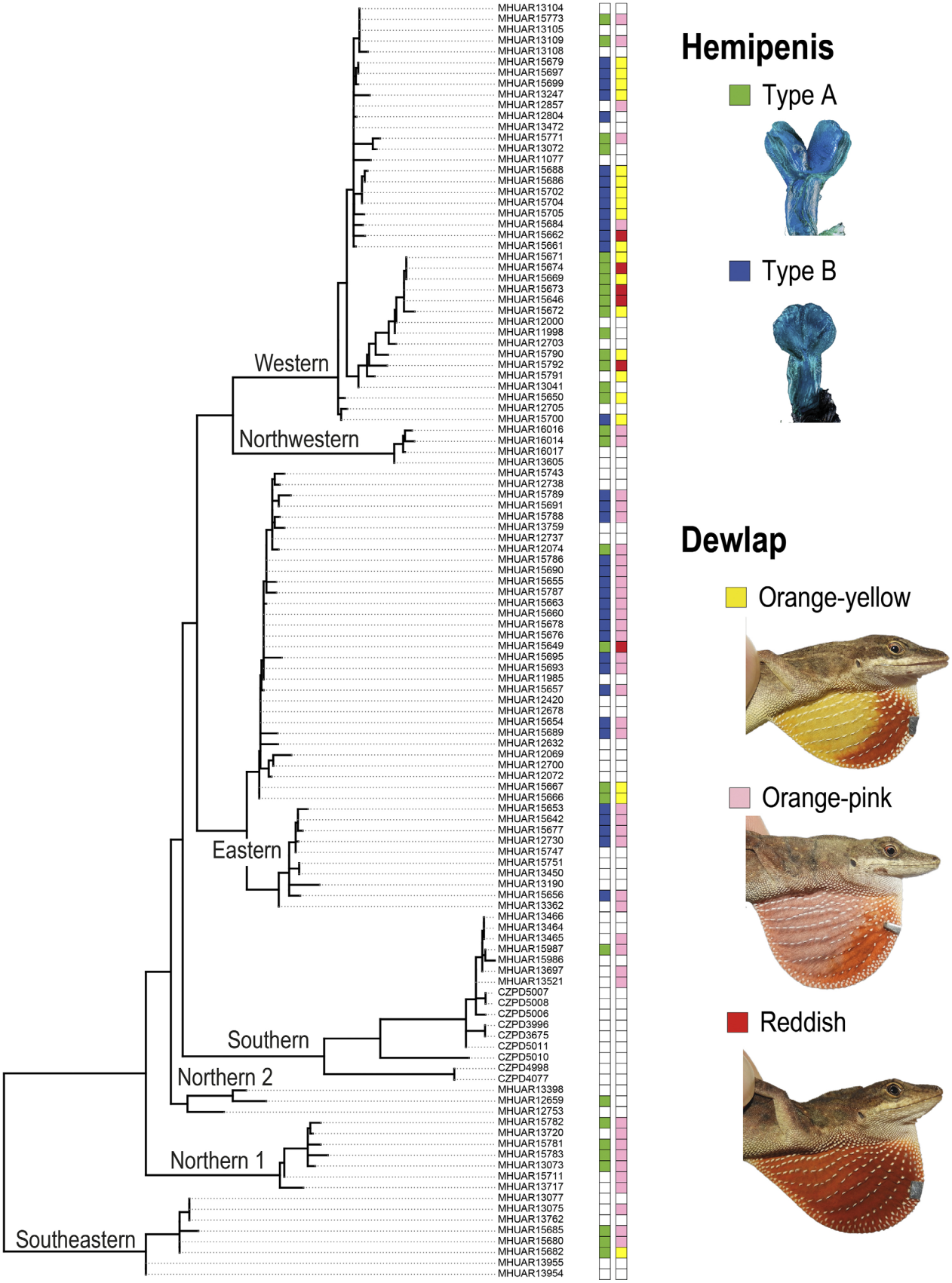

Figure 2. Hemipenis and dewlap character states mapped onto the ML tree presented in Figure 1. White boxes indicate females or undetermined state.

for type B. Hemipenial type A exhibited a broader distribution, occurring on both sides of the Cauca River Valley in the Central and Western Andes, as well as on both sides of the Medellín River Valley in the Central Andes. In contrast, type B was mainly restricted to areas south of the Medellín River Valley in the Central Andes (Fig. 3).

Table 1. Simple of molecular variance AMOVA for testing the genetic subdivision of dewlap colour pattern, hemipenial morphs and clades of *A. mariarum* using nucleotide sequence of mitochondrial 16S, cyt *b* and ND2 regions.

Source of variation	d.f.	Sum of squares	Variance components	% of variation	F-statistics
			16S		
Dewlap colour pattern					
Among populations	3	315,628	1966	2790	Φst=0.02790, p<0.127
Within populations	52	3,562,158	68,503	97,210	
Total	55	3,877,786	70,469		
Hemipenis morphs					
Among populations	2	327,766	3494	4899	Φst=0.04899, p<0.023
Within populations	52	3,526,197	67,811	95,101	
Total	54	3,853,964	71,305		
			Clades		
Among populations	6	3,689,932	66,717	95,127	Φst=0.95127, p<0.001
Within populations	48	164,032	3417	4873	
Total	54	3,853,964	70,134		
			cyt *b*		
Dewlap colour pattern					
Among populations	3	2,199,741	23,891	8092	Φst=0.08092, p<0.002
Within populations	54	14,653,431	271,360	91,908	
Total	57	16,853,172	295,251		
Hemipenis morphs					
Among populations	2	1,504,993	16,477	5504	Φst=0.05504, p<0.015
Within populations	54	15,275,972	282,888	94,496	
Total	56	16,780,965	299,366		
			Clades		
Among populations	5	15,829,674	276,077	93,671	Φst=0.93671, p<0.001
Within populations	51	951,291	18,653	6329	
Total	56	16,780,965	294,730		
			ND2		
Dewlap colour pattern					
Among populations	3	4,038,884	31,682	5219	Φst=0.05219, p<0.007
Within populations	69	39,700,966	575,376	94,781	
Total	72	43,739,849	607,058		
			Hemipenis morphs		
Among populations	2	2,446,724	18,015	3039	Φst=0.03039, p<0.038
Within populations	69	39,663,734	574,837	96,961	
Total	71	42,110,458	592,851		
			Clades		
Among populations	6	36,320,078	488,295	81,286	Φst=0.81286, p<0.001
Within populations	66	7,419,771	112,421	18,714	
Total	72	43,739,849	600,716		

Genetic structure

After constructing a TCS network with the cyt *b* gene, we found 40 private haplotypes and eight common haplotypes, present in between two and seven individuals. (Fig. 4). In the other two regions, lesser haplotype diversity was observed, with 16 private and nine shared haplotypes in 16S (2 to 16 individuals), and 16 private and 13 shared haplotypes in ND2 (2 to 24 individuals; Figs S6–S11). There is no apparent link between traits and haplotypes in any mitochondrial gene (16S, ND2, and cyt *b*). Both hemipenial morphs and all three dewlap colour share haplotypes (Figs 4, S6, S7, S9, S10). For the cyt *b* gene, haplotypes are grouped into seven distinct clusters with multiple mutations and missing haplotypes between them (Fig. S12). The eastern and western haplogroups show the highest haplotype diversity, with 18 and 15 haplotypes, respectively (Fig. S12).

AMOVA showed that most genetic variation was explained by differences among clades (16S: 95.1%, cyt *b*: 93.7%, ND2: 81.3%; p = 0.001). In contrast, grouping by dewlap colour pattern or hemipenial morphology revealed that most variation occurred within groups rather than among them (generally >90% across loci, with variable significance) (Table 1). Genetic differentiation indices (G_{ST}, N_{ST}, Φ_{ST}; Table S3) further indicate strong divergence among clades, with N_{ST} consistently higher than G_{ST}, supporting a marked phylogeographic structure. Φ_{ST} values were high across loci (16S: 0.677–0.971; cyt *b*: 0.743–0.965; ND2: 0.404–0.980). Additionally,

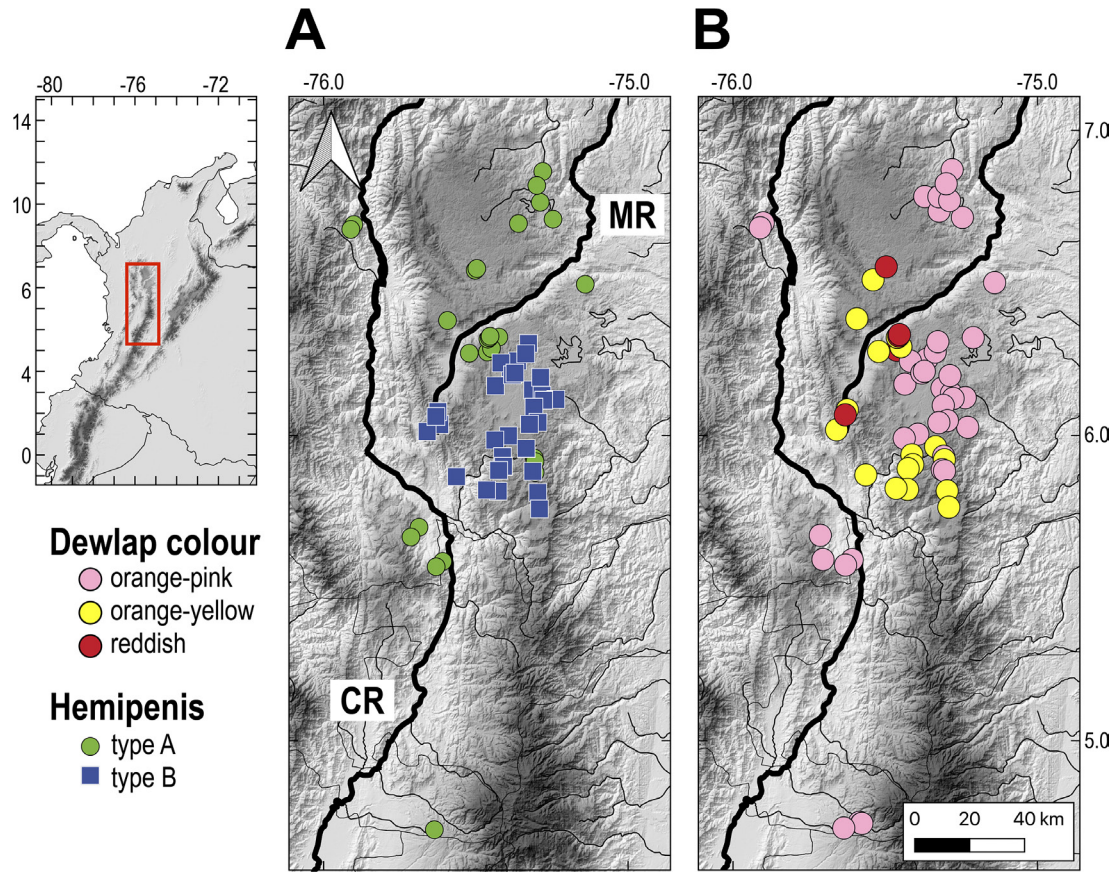

Figure 3. Geographic location of hemipenial morphology (**A**) and dewlap colour pattern (**B**) of *A. mariarum*. CR: Cauca River, MR: Medellín River.

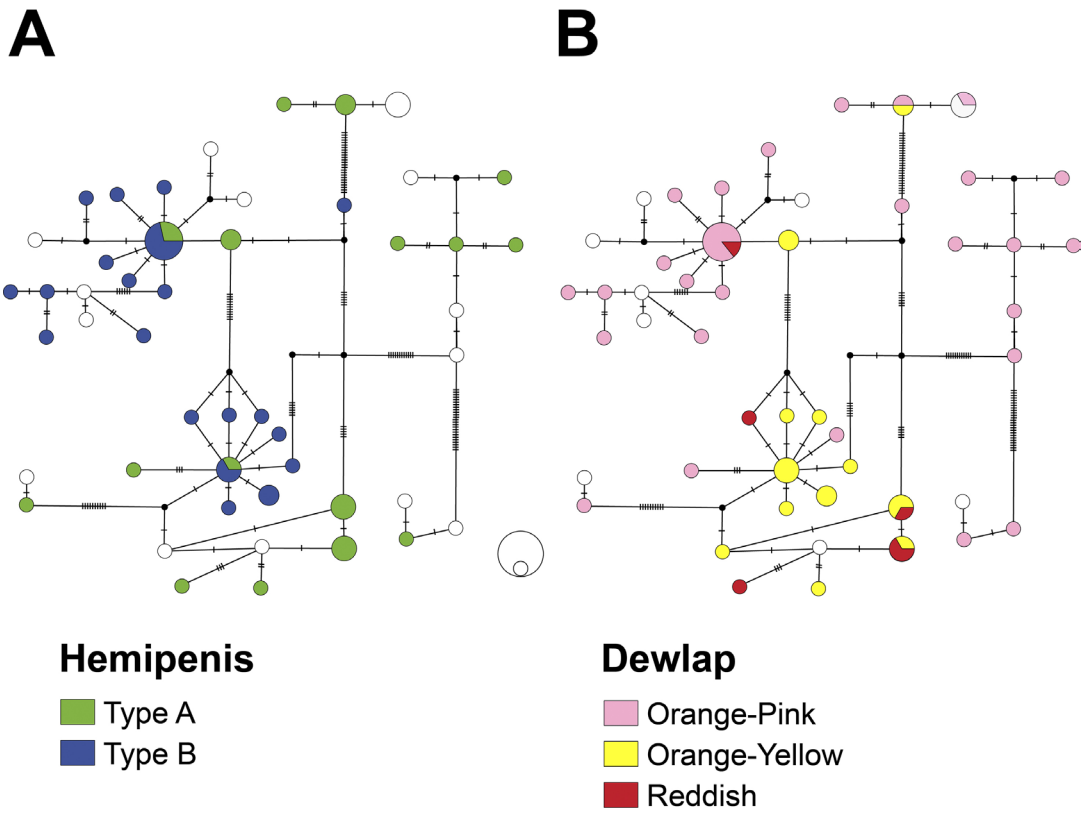

Figure 4. TCS network for hemipenial morphs (**A**) and dewlap colour pattern (**B**) in *A. mariarum*, based on 800 bp of the cyt *b* gene. The colour code represents trait states, and circle size reflects haplotype frequency (large circle corresponding to 10 samples and smaller inner circle representing a single sample). White circles indicate females or individuals with unknown trait states. Missing haplotypes are represented by black dots, and the bars across the lines connecting haplotypes correspond to one mutational step.

cyt *b* showed higher nucleotide divergence (K_{XY}, D_{XY}) than 16S and ND2 (Table S3). Overall, the southeastern clade was the most differentiated, whereas the western and northern_2 clades showed lower differentiation with the eastern and northwestern clades.

Finally, mean uncorrected genetic distances between mitochondrial clades varied among the three mitochondrial markers (Table S4). For the 16S marker, inter-clade genetic distances ranged from 1.4% to 4.4%, with the lowest divergence observed between the eastern and northern (northern_1 and northern_2) clades and the highest between the northern_1 and southern clades. For ND2, genetic distances ranged from 1.9% to 7.1%, with the greatest divergence involving the southeastern clade. Similarly, cyt *b* exhibited inter-clade genetic distances ranging from 2.2% to 5.9%, with the highest divergence recorded between the southeastern and southern clades.

Discussion

The integrative analyses in this study reveal that *Anolis mariarum* exhibits a complex pattern of evolutionary diversification, where deep phylogeographic structure coexists with marked phenotypic variation. As a starting point to understand this intraspecific variation, we first established the evolutionary neighborhood of *A. mariarum* by clarifying its relationships with closely related species. Although genetic lineages within our focal species are strongly structured across the Central and Western Andes, both dewlap colour and hemipenial morphology show a significant phylogenetic signal, indicating that their variation is not random with respect to evolutionary history. However, this signal does not translate into a clear correspondence, as these traits broadly overlap in geographic space.

Evolutionary relationships and phylogeography

This study provides new insights into the evolutionary relationships and distribution of *Anolis mariarum*. Contrary to previous hypotheses (Poe et al. 2015; Grisales-Martínez et al. 2017; Poe et al. 2017), our results recover *A. tolimensis* as the sister species of *A. mariarum*, rather than *A. antonii*, which is instead nested within a clade of Central American *fuscoauratus*-like species (Files S12–14). These findings highlight the importance of incorporating topotypic material when resolving taxonomically challenging and potentially cryptic species complexes (e.g., Grisales-Martínez et al. 2017; Townsend and Hofmann 2017; Marín et al. 2025). We confirmed the presence of *A. mariarum* in the northern Western Andes of Antioquia and extended its known distribution to Quindío, Risaralda, and Valle del Cauca. Specimens from these regions correspond to the southern clade and had previously been attributed to *A. antonii* (Fig. 1; Rojas-Morales et al. 2014; López-Herrera et al. 2016; Grisales-Martínez et al. 2017; Moreno-Arias et al. 2021), suggesting that some historical records of *A. antonii* actually represent populations of *A. mariarum*. We also ruled out the presence of *A. tolimensis* in Antioquia (Páez et al. 2002), as earlier records for this species, documented by Williams in "New or Problematic *Anolis* from Colombia VII", were based on specimens from eastern Antioquia, located 180 km from the species' type locality in the Combeima Canyon, Tolima. These specimens, however, belong to the eastern clade of *A. mariarum* rather than to *A. tolimensis* (see Poe et al. 2015). Our extensive sampling of *A. mariarum* has expanded the known distribution of the species, which ranges from 1000 to 2620 meters in elevation, with occurrences at lower altitudes, particularly in the Western Andean.

Having clarified the species boundaries of *A. mariarum*, we now turn to its internal phylogeographic structure. Our analysis revealed seven mitochondrial clades in *Anolis mariarum*, with a partially structured phylogeographic pattern (Fig. 1). Some clades are clearly associated with Andean geography: for example, the northwestern clade in the Western Andes, and the eastern and southeastern clades in the Central Andes south of the Medellín River, while northern_1 and northern_2 occur north of this river. This pattern is consistent with the role of Andean mountain systems and inter-Andean valleys as barriers to gene flow, as documented in multiple vertebrate groups (e.g., Cadena et al. 2019; Ruiz-García et al. 2020; Arbeláez-Cortés and Trujillo-Arias 2021; Genty et al. 2022; Rivera-Correa et al. 2022). However, other clades do not follow these geographic divisions: the southern and western clades occur across both the Western and Central Andes, including both sides of the Medellín River (Fig. 1). This result may indicate recent historical connections or gene flow between these mountain ranges. This is supported by evidence that in Neotropical species, topography not only plays a significant role but also interacts with historical climate, contributing to the emergence of complex phylogeographic patterns (Daza et al. 2009; Ávila-Lovera et al. 2024). Nevertheless, these phylogeographic inferences should be interpreted with caution because they are based exclusively on mitochondrial markers. As mtDNA reflects only the maternal evolutionary history, the identified clades should be regarded as mitochondrial lineages rather than definitive independently evolving lineages, since processes such as incomplete lineage sorting or introgression may lead to discordance between mitochondrial and genome-wide patterns of divergence.

Hemipenial evolution

This study represents the most comprehensive intraspecific assessment of hemipenial variation in *Anolis* to date, based on the examination of 65 individuals across 26 localities within an explicit evolutionary framework. We identified two distinct bilobed hemipenial morphs (type A and type B) with clear morphological differences and unrelated to allometry: type A is more developed, with a thicker trunk and larger lobes, whereas type B is smaller and less developed (Figs S1, S2). These results contrast

with those of Melo-Torres et al. (2025), who proposed a third morphotype based on a more limited sample, which was not detected in our study. Given that hemipenial morphology in anoles is a rapidly evolving trait associated with divergence, reproductive isolation, and lineage formation, and has been key in distinguishing closely related species (Köhler et al. 2010, 2012a, 2012b; Klaczko et al. 2015; D'Angiolella et al. 2016), the patterns observed in *A. mariarum* are particularly informative.

Hemipenial morphology exhibited a strong phylogenetic signal, indicating that closely related populations possess more similar hemipenial morphologies than expected by chance (Fig. S5). This result suggests that hemipenial variation may track evolutionary divergence among populations and highlights its potential relevance to the early stages of reproductive diversification in *Anolis*. In anoles, differences in hemipenial morphology could contribute to reproductive isolation through mechanical incompatibility or differences in copulatory interactions, thereby facilitating divergence when populations become genetically or geographically differentiated. However, in *A. mariarum*, the absence of a direct correspondence between hemipenial morphs and mitochondrial lineages indicates that hemipenial divergence alone is not sufficient to infer ongoing speciation (Figs 4, S6, S9, Table 1). Rather, the strong phylogenetic signal suggests that this reproductive trait may respond to evolutionary divergence at a different tempo from neutral mitochondrial markers. The combination of strong phylogenetic signal with shallow mitochondrial divergence is therefore consistent with the possibility that reproductive traits may diverge early during lineage diversification, potentially preceding detectable differentiation in neutral markers. This hypothesis is particularly relevant to anoles, where reproductive trait divergence may contribute to the establishment or maintenance of reproductive barriers among geographically structured populations. Nevertheless, testing whether hemipenial divergence contributes directly to speciation in *A. mariarum* will require evidence of reproductive isolation, gene flow, and genome-wide differentiation.

Dewlap evolution

The variation observed in *Anolis mariarum* represents the most diverse range of dewlap patterns and colour documented for any *Anolis*, whether continental or insular, within a relatively small spatial scale. In this species, we identified three dewlap colour patterns—two divided (orange-yellow and orange-pink; Grisales-Martínez et al. 2017) and one solid, a newly documented uniform reddish morph (Fig. S3)—a level of diversity that becomes even more striking when compared with other species. For example, *Anolis fuscoauratus* D'Orbigny, 1837 in South America has one solid dewlap pattern with three colour variants (Prates et al. 2021), while *Anolis apletophallus* Köhler & Sunyer, 2008 in Central America shows two dewlap patterns with two colour variants (Stapley et al. 2011). *Anolis distichus* Cope, 1861 in the Caribbean spans a much larger range (about 80,000 km²) and exhibits two dewlap patterns with extensive colour diversity (Ng and Glor 2011). In contrast, the sampled range for *A. mariarum* in this study covers only about 15,000 km², yet it includes two distinct dewlap patterns and three-colour variants, showcasing the exceptional diversity of this trait within the species.

Dewlap variation in anoles is often linked to geographic structure, genetic differentiation, reproductive isolation or environmental adaptation (Leal and Fleishman 2004; Ng et al. 2013; Prates et al. 2021). In *Anolis mariarum*, molecular evidence indicates that individuals sharing the same dewlap colour pattern do not exhibit marked genetic differentiation (Figs 4, S7, S10; Table 1). Several alternative explanations for this diversity can also be ruled out. Spatial analyses further reveal no spatial correlation or geographic structuring of dewlap morphotypes across the heterogeneous Andean landscape. Character displacement also appears unlikely, as *A. mariarum* coexists with other *Anolis* species occupying distinct habitats and displaying different dewlap colour patterns (e.g., *Anolis quimbaya* Moreno-Arias et al., 2023; *Anolis eulaemus* Boulenger, 1908; *Anolis ventrimaculatus* Boulenger, 1911). Moreover, dewlap morphotypes frequently occur in the same or adjacent localities with similar open vegetation cover (the preferred habitat of the species) suggesting that signal optimization for contrasting environments is not a major driver.

Despite the absence of clear mitochondrial or geographic structuring, dewlap coloration also exhibited a strong phylogenetic signal, indicating that closely related populations tend to resemble each other in dewlap coloration more than expected by chance (Fig. S5). This phylogenetic signal suggests that dewlap colour variation is associated with evolutionary history and may accumulate during population divergence rather than arising repeatedly through independent evolution. Such a pattern is particularly relevant to speciation because sexually selected traits can diverge among populations and subsequently contribute to prezygotic isolation through differences in mate recognition or preference. However, because mitochondrial genetic differentiation among clades is shallow, the observed pattern is more consistent with an early stage of divergence in which a reproductively relevant phenotype may begin to differentiate while neutral genetic differentiation remains limited. Therefore, our results do not demonstrate that dewlap divergence is driving speciation in *A. mariarum*, but they identify dewlap coloration as a potential component of the phenotypic divergence that could contribute to reproductive isolation in continental *Anolis*. As with hemipenial divergence, confirming this role will require evaluating mate preferences, signal perception, gene flow, and genome-wide differentiation among dewlap morphotypes.

Genetic divergence and evolutionary implications

This study provides the first comprehensive assessment of genetic diversity and population structure in a South American Andean *Anolis*, supported by robust geo-

graphic and multilocus sampling using three mitochondrial markers. A strong genetic structure was detected in *A. mariarum*, largely aligned with mtDNA clades, which better explain the observed genetic variation than phenotypic traits such as dewlap colour pattern and hemipenial morphology. A key contribution of this study is the inclusion of cyt *b*, a gene not previously applied in continental South American anoles, which proved to be the most variable and informative marker, showing the highest number of haplotypes (Figs 4, S12) and greater differentiation indices (Φ_{ST}, K_{XY}, D_{XY}) among clades (Table S3). High Φ_{ST} values among clades, together with N_{ST} consistently exceeding G_{ST}, support pronounced genetic structure, indicating that haplotypes within clades are more closely related to each other than to those from other clades (Pons and Petit 1996). Although Φ_{ST} values for haploid data may overestimate differentiation compared to F_{ST} (Excoffier 2007), they remain a valuable metric for group comparisons (Fratini et al. 2016; Ng et al. 2016; Hernández-Rangel et al. 2024). Additionally, AMOVA results show that variation among populations is best explained by mtDNA clades, whereas variation within populations is associated with phenotypic traits (Table 1). This reliance on a single mitochondrial marker warrants caution, as its the scope and limitations of mtDNA have been discussed in recent literature (Wüster 2025). Nonetheless, mtDNA continues to represent a powerful and widely used marker for formulating primary hypotheses on intra- and interspecific relationships and boundaries (Blair 2023).

The levels of mitochondrial divergence observed among some *Anolis mariarum* clades are comparable to values reported for taxonomic units recognized as subspecies and, in some cases, even distinct species. For the ND2 marker, the highest inter-clade divergences (6.4–7.1%) overlapped with values reported among subspecies of the *Anolis distichus* complex, including 2.3% between *Anolis distichus ignigularis* Mertens, 1939, and *Anolis distichus ravitergum* Schwartz, 1968, and 7.7% between *A. d. ravitergum* and *Anolis distichus properus* Schwartz, 1968 (Glor and Laport 2012), as well as the 6.2–7.5% divergence reported between mainland populations of *Anolis carolinensis* Voigt, 1832, and the peninsular subspecies *A. carolinensis seminolus* Vance, 1991 (Tollis et al. 2012). Likewise, several pairwise comparisons among *A. mariarum* clades exceeded 2% for the more conserved 16S marker (2.5–4.4%), overlapping the 2–4% interspecific divergences reported for members of the *Anolis latifrons* series (Marín et al. 2025).

Collectively, these findings demonstrate that mitochondrial DNA, particularly cyt *b*, is highly effective for detecting phylogeographic structure and historical population differentiation in *Anolis mariarum*. Although based on a single, maternally inherited genomic compartment, the concordance among mitochondrial markers and the magnitude of the observed genetic divergence provides strong evidence for deep evolutionary subdivision within the species. These results establish an important foundation for future studies integrating genomic and ecological data to further elucidate the evolutionary history and diversification of *A. mariarum* and other Neotropical *Anolis* species.

Conclusions

Our results reveal a striking combination of phylogeographic structure, morphological polymorphism, and phylogenetic signal across populations of *Anolis mariarum*, highlighting a dynamic evolutionary scenario within this Andean lineage. The concordance between geographically structured genetic variation and divergence in key reproductive and signaling traits suggests that these characters are not evolving randomly but instead may be associated with processes of population differentiation. However, because these inferences are based exclusively on mtDNA, alternative evolutionary processes, including incomplete lineage sorting, retention of ancestral polymorphism, recent divergence without reproductive isolation, or introgression, cannot be ruled out. The presence of polymorphism in traits typically involved in species recognition supports the hypothesis that these traits may be involved in evolutionary diversification, although their relationship with lineage divergence requires confirmation using nuclear genomic data. Together, these patterns provide a preliminary evolutionary framework for understanding the interaction between phenotypic and mitochondrial variation in *A. mariarum* and generate testable hypotheses about the processes shaping diversification in this Andean lineage.

Acknowledgements

We thank the following biologists for their suggestions and for sharing photographic dewlap records: Beatriz Elena Rendón, Paola Martínez, Viviana Cartagena, Alejandro Montoya, Carlos Marín, Diego Alzate, Diego Rivera, Edilson Garcés, Esteban Alzate, Juan Pablo Hurtado, Mauricio Rivera, Yeison Tolosa, and Wilmar Agudelo. We thank Duvan Zambrano for his guidance in hemipenial preparation, Santiago Varela for hemipenial photographs, and Katherine Rodríguez for assistance with morphometric data. We are grateful to the Museo de Herpetología Universidad de Antioquia (MHUA) and to Carolina Torres for assistance with laboratory work. Financial support was provided by Servicios Ambientales y Geográficos S.A. and the Universidad de Antioquia. We further thank Catalina González, Edward Myers, Rafael Moreno, Carlos Pavón, and the anonymous reviewers for their valuable comments. The first author is especially grateful to his life partner Betty, for her invaluable contributions to specimen collection, sample preparation, and the development of this research. He also thanks his son Dante, whose joyful presence provided constant inspiration and motivation during the final stages of this study.

References

Anselin L (1995) Local indicators of spatial association – LISA. Geographical Analysis 27: 93–115. https://doi.org/10.2307/2332142

Arbeláez-Cortés E, Trujillo-Arias N (2021) Role of the Chicamocha River Canyon on the phylogeography of humid montane forest birds in Colombia. Journal of Avian Biology 52: 1–10. https://doi.org/10.1111/jav.02833

Ávila-Lovera E, Vargas OM, Funk JL, Kay KM, Goldsmith GR (2024) Climate and shared evolutionary history drive trait variation among

species of Neotropical understory monocots. Ecosphere 15: e4880. https://doi.org/10.1002/ecs2.4880

Bateman RM, DiMichele WA (2002) Generating and filtering major phenotypic novelties: NeoGoldschmidtian saltation revisited. In: Cronk QCB, Bateman RM, Hawkins JA (Eds) Developmental Genetics and Plant Evolution. Taylor & Francis, London, 109–159.

Blair C (2023) Organellar DNA continues to provide a rich source of information in the genomics era. Molecular Ecology 32: 2144–2150. https://doi.org/10.1111/mec.16872

Bivand R, Altman M, Anselin L, Assunção R, Berke O, Bernat A, Blanchet G (2017) spdep: Spatial dependence: Weighting schemes, statistics, R package version, 1-1.2017. https://CRAN.R-project.org/package=spdep

Blomberg SP, Garland TJr, Ives AR (2003) Testing for phylogenetic signal in comparative data: Behavioral traits are more labile. Evolution 57: 717–745. https://doi.org/10.1111/j.0014-3820.2003.tb00285.x

Borges R, Machado JP, Gomes C, Rocha AP, Antunes A (2019) Measuring phylogenetic signal between categorical traits and phylogenies. Bioinformatics 35: 1862–1869. https://doi.org/10.1093/bioinformatics/bty800

Cadena CD, Pérez-Eman JL, Cuervo AM, Céspedes LN, Epperly KL, Klicka JT (2019) Extreme genetic structure and dynamic range evolution in a montane passerine bird: Implications for tropical diversification. Biological Journal of the Linnean Society 126: 487–506. https://doi.org/10.1093/biolinnean/bly207

Castañeda MR, de Queiroz K (2011) Phylogenetic relationships of the *Dactyloa* clade of *Anolis* lizards based on nuclear and mitochondrial DNA sequence data. Molecular Phylogenetics and Evolution 61: 784–800. https://doi.org/10.1016/j.ympev.2011.07.004

Clement M, Posada D, Crandall KA (2000) TCS: A computer program to estimate gene genealogies. Molecular Ecology 9: 1657–1659. https://doi.org/10.1046/j.1365-94x.2000.01020.x

D'Angiolella AB, Klaczko J, Rodrigues MT, Avila-Pires TCS (2016) Hemipenial morphology and diversity in South American anoles (Squamata: Dactyloidae). Canadian Journal of Zoology 94: 251–256. https://doi.org/10.1139/cjz-2015-0194

Daza JM, Smith EN, Páez VP, Parkinson CL (2009) Complex evolution in the Neotropics: The origin and diversification of the widespread genus *Leptodeira* (Serpentes: Colubridae). Molecular Phylogenetics and Evolution 53: 653–667. https://doi.org/10.1016/j.ympev.2009.07.022

Excoffier L (2007) Analysis of population subdivision. In: Balding DJ, Bishop M, Cannings C (Eds) Chichester Handbook of Statistical Genetics. John Wiley & Sons, Hoboken, NJ, 271–307.

Excoffier L, Smouse PE, Quattro JM (1992) Analysis of molecular variance inferred from metric distance among DNA haplotypes: Application to human mitochondrial DNA restriction data. Genetics 131: 479–491. https://doi.org/10.1093/genetics/131.2.479

Fratini S, Ragionieri L, Deli T, Harrer A, Marino IA, Cannicci S, Zane L, Schubart CD (2016) Unravelling population genetic structure with mitochondrial DNA in a notional panmictic coastal crab species: Sample size makes the difference. BMC Evolutionary Biology 16: 150. https://doi.org/10.1186/s12862-016-0720-2

Fusco G, Minelli A (2010) Phenotypic plasticity in development and evolution: Facts and concepts. Philosophical Transactions of the Royal Society B 365: 547–556. https://doi.org/10.1098/rstb.2009.0267

Gallant JR, O'Connell LA (2020) Studying convergent evolution to relate genotype to behavioral phenotype. Journal of Experimental Biology 223: jeb213447. https://doi.org/10.1242/jeb.213447

Genty G, Guarnizo CE, Ramírez JP, Barrientos LS, Crawford AJ (2022) Landscape genetics and species delimitation in the Andean palm rocket frog (Aromobatidae, *Rheobates*). Journal of Zoological Systematics and Evolutionary Research 2022: 774225. https://doi.org/10.1155/2022/6774225

Gilman CA, Corl A, Sinervo B, Irschick DJ (2019) Genital morphology associated with mating strategy in the polymorphic lizard, *Uta stansburiana*. Journal of Morphology 280: 184–192. https://doi.org/10.1002/jmor.20930

Glor RE, Laport RG (2012) Are subspecies of *Anolis* lizards that differ in dewlap color and pattern also genetically distinct? A mitochondrial analysis. Molecular Phylogenetics and Evolution 64: 255–260. https://doi.org/10.1016/j.ympev.2010.11.004

Goebel AM, Donnelly JM, Atz ME (1999) PCR primers and amplification methods for 12S ribosomal DNA, the control region, cytochrome oxidase I, and cytochrome *b* in bufonids and other frogs, and an overview of PCR primers which have amplified DNA in amphibians successfully. Molecular Phylogenetics and Evolution 11: 163–199. https://doi.org/10.1006/mpev.1998.0538

Grisales-Martinez FA, Velasco JA, Bolivar W, Williams EE, Daza JM (2017) The taxonomic and phylogenetic status of some poorly known *Anolis* species from the Andes of Colombia with the description of a *nomen nudum* taxon. Zootaxa 4303: 213–230. https://doi.org/10.11646/zootaxa.4303.2.2

Harris RB, Alström P, Ödeen A, Leaché AD (2018) Discordance between genomic divergence and phenotypic variation in a rapidly evolving avian genus (*Motacilla*). Molecular Phylogenetics and Evolution 120: 183–195. https://doi.org/10.1016/j.ympev.2017.11.020

Hernández-Rangel SM, Morales-Betancourt MA, Muniz FL, Vargas-Ramírez M, Rojas-Runjaic FJ, Lasso CA, Caballero S (2024) Phylogenetic identity and population structure of the dwarf caimans *Paleosuchus* spp. in the Orinoco basin of Colombia and Venezuela: Filling gaps. Biological Journal of the Linnean Society 142: 68–80. https://doi.org/10.1093/biolinnean/blad145

Hernández-Salinas U, Ramírez-Bautista A, Pavón NP, Rosas-Pacheco LF (2014) Morphometric variation in island and mainland populations of two lizard species from the Pacific Coast of Mexico. Revista Chilena de Historia Natural 87: 21. https://doi.org/10.1186/S40693-014-0021-3

Hoang DT, Chernomor O, von Haeseler A, Minh BQ, Vinh LS (2018) UFBoot2: Improving the ultrafast bootstrap approximation. Molecular Biology and Evolution 35: 518–522. https://doi.org/10.1093/molbev/msx281

Jacobs JA, Salazar JC, Winchell KM (2023) A picture is worth a thousand dollars: A photographic approach to studying colour in anoles. Biological Journal of the Linnean Society 142: 319–330. https://doi.org/10.1093/biolinnean/blad143

Jiménez RA (2021) Biogeography and Evolution of Montane Birds across Nuclear Central America. Chapter 2: Elucidation of the phylogeography and genetic basis of phenotype-genotype discordance in the white-naped brushfinch (*Atlapetes albinucha*) across its geographic range. PhD Thesis, University of California, Berkeley, CA, 206 pp.

Jombart T (2008) Adegenet: A R package for the multivariate analysis of genetic markers. Bioinformatics 24: 1403–1405. https://doi.org/10.1093/bioinformatics/btn129

Jombart T, Devillard S, Balloux F (2010) Discriminant analysis of principal components: A new method for the analysis of genetically structured populations. BMC Genetics 11: 94. https://doi.org/10.1186/1471-2156-11-94

Kalyaanamoorthy S, Minh BQ, Wong TK, von Haeseler A, Jermiin LS (2017) ModelFinder: Fast model selection for accurate phylogenetic estimates. Nature Methods 14: 587–589. https://doi.org/10.1038/nmeth.4285

Katoh K, Standley DM (2013) MAFFT multiple sequence alignment software version 7: Improvements in performance and usability. Molecular Biology and Evolution 30: 772–780. https://doi.org/10.1093/molbev/mst010

Klaczko J, Ingram T, Losos J (2015) Genitals evolve faster than other traits in *Anolis* lizards. Journal of Zoology 295: 44–48. https://doi.org/10.1111/jzo.12178

Köhler G (2012) Color Catalogue for Field Biologists. Herpeton, Offenbach, 49 pp.

Köhler G, Batista A, Vesely M, Ponce M, Carrizo A, Lotzkat S (2012b) Evidence for the recognition of two species of *Anolis* formerly referred to as *A. tropidogaster* (Squamata: Dactyloidae). Zootaxa 3348: 1–23. https://doi.org/10.11646/zootaxa.3348.1.1

Köhler G, Dehling DM, Köhler J (2010) Cryptic species and hybridization in the *Anolis polylepis* complex, with the description of a new species from the Osa Peninsula, Costa Rica (Squamata: Polychrotidae). Zootaxa 2718: 23–38. https://doi.org/10.11646/zootaxa.2718.1.2

Köhler G, Vargas J (2019) A new species of anole from Parque Nacional Volcán Arenal, Costa Rica (Reptilia, Squamata, Dactyloidae: *Norops*). Zootaxa 4608: 261–278. https://doi.org/10.11646/zootaxa.4608.2.4

Köhler J, Hahn M, Köhler G (2012a) Divergent evolution of hemipenial morphology in two cryptic species of mainland anoles related to *Anolis polylepis*. Salamandra 48: 1–11.

Lalejini A, Ferguson AJ, Grant NA, Ofria C (2021) Adaptive phenotypic plasticity stabilizes evolution in fluctuating environments. Frontiers in Ecology and Evolution 9: 715381. https://doi.org/10.3389/fevo.2021.715381

Lanfear R, Calcott B, Ho SY, Guindon S (2012) PartitionFinder: Combined selection of partitioning schemes and substitution models for phylogenetic analyses. Molecular Biology and Evolution 29: 1695–1701. https://doi.org/10.1093/molbev/mss020

Leal M, Fleishman LJ (2004) Differences in visual signal design and detectability between allopatric populations of *Anolis* lizards. American Naturalist 163: 26–39. https://doi.org/10.1086/379794

Leigh JW, Bryant D (2015) POPART: Full-feature software for haplotype network construction. Methods in Ecology and Evolution 6: 1110–1116. https://doi.org/10.1111/2041-210X.12410

Librado P, Rozas J (2009) DnaSP v5: A software for comprehensive analysis of DNA polymorphism data. Bioinformatics 25: 1451–1452. https://doi.org/10.1093/bioinformatics/btp187

López-Herrera DF, León-Yusti M, Guevara-Molina SC, Vargas-Salinas F (2016) Reptiles en corredores biológicos y mortalidad por atropellamiento vehicular en Barbas-Bremen, Quindío, Colombia. Revista de la Academia Colombiana de Ciencias Exactas, Físicas y Naturales 40: 484–493. https://doi.org/10.18257/raccefyn.334

Losos JB (2008) Phylogenetic niche conservatism, phylogenetic signal and the relationship between phylogenetic relatedness and ecological similarity among species. Ecology Letters 11: 995–1003. https://doi.org/10.1111/j.1461-0248.2008.01229.x

Losos JB, Schneider CJ (2009) *Anolis* lizards. Current Biology 19: R316–R318.

Macey JR, Larson A, Ananjeva NB, Fang Z, Papenfuss TJ (1997) Two novel gene orders and the role of light-strand replication in rearrangement of the vertebrate mitochondrial genome. Molecular Biology and Evolution 14: 91–104. https://doi.org/10.1093/oxfordjournals.molbev.a025706

Marín CM, Bocanumenth D, Daza JM (2025) The colorful giants: Revisiting the systematics of the *Anolis latifrons* series (Squamata: Anolidae). Vertebrate Zoology 75: 441–457. https://doi.org/10.3897/vz.75.e162071

Márquez R, Linderoth TP, Mejía-Vargas D, Nielsen R, Amézquita A, Kronforst MR (2020) Divergence, gene flow, and the origin of leapfrog geographic distributions: The history of colour pattern variation in *Phyllobates* poison-dart frogs. Molecular Ecology 29: 3702–3719. https://doi.org/10.1111/mec.15598

Melo-Torres S, Uchima J, Pinto-Sánchez N, Sánchez-Martínez P (2025) Morphological description and ancestral state reconstruction of the hemipenes of five *Anolis* species (Squamata: Dactyloidae) distributed in the trans-Andean region in Colombia. Revista Latinoamericana de Herpetología 8: 230–253. https://doi.org/10.22201/fc.25942158e.2025.2.1140

Moreno-Arias RA, Velasco JA, Urbina-Cardona JN, Cárdenas-Arévalo G, Medina-Rangel GF, Gutiérrez-Cárdenas PDA, Olaya-Rodríguez MH, Cruz-Rodríguez C, Noguera-Urbano E (2021) Atlas de la biodiversidad de Colombia. *Anolis*. Instituto de Investigación de Recursos Biológicos Alexander von Humboldt, Bogotá, 72 pp.

Moritz C, Schneider CJ, Wake DB (1992) Evolutionary relationships within the *Ensatina eschscholtzii* complex confirm the ring species interpretation. Systematic Biology 41: 273–291. https://doi.org/10.1093/sysbio/41.3.273

Ng J, Geneva AJ, Noll S, Glor RE (2017) Signals and speciation: *Anolis* dewlap color as a reproductive barrier. Journal of Herpetology 51: 437–447. https://doi.org/10.1670/16-033

Ng J, Glor RE (2011) Genetic differentiation among populations of a Hispaniolan trunk anole that exhibit geographical variation in dewlap colour. Molecular Ecology 20: 4302–4317. https://doi.org/10.1111/j1365-294X.2011.05267.x

Ng J, Landeen EL, Logsdon RM, Glor RE (2013) Correlation between *Anolis* lizard dewlap phenotype and environmental variation indicates adaptive divergence of a signal important to sexual selection and species recognition. Evolution 67: 573–582. https://doi.org/10.1111/j.1558-5646.2012.01795.x

Ng J, Ossip-Klein AG, Glor RE (2016) Adaptive signal coloration maintained in the face of gene flow in a Hispaniolan *Anolis* lizard. BMC Evolutionary Biology 16: 193. doi.org/10.1186/s12862-016-0763-4

Nguyen LT, Schmidt HA, Von Haeseler A, Minh BQ (2015) IQ-TREE: A fast and effective stochastic algorithm for estimating maximum-likelihood phylogenies. Molecular Biology and Evolution 32: 268–274. https://doi.org/10.1093/molbev/msu300

Nicholson KE, Harmon LJ, Losos JB (2007) Evolution of *Anolis* lizard dewlap diversity. PLoS One 2: e274. https://doi.org/10.1371/journal.pone.0000274

Orgogozo V, Morizot B, Martin A (2015) The differential view of genotype–phenotype relationships. Frontiers in Genetics 6: 1–14. https://doi.org/10.3389/fgene.2015.00179

Páez VP, Bock BC, Ortega AM, Estrada JJ, Daza JM (2002) Guía de campo de algunas especies de anfibios y reptiles de Antioquia. Multimpresos Ltda, Medellín, 136 pp.

Palumbi SR (1996) Nucleic acids II: The polymerase chain reaction. In: Hillis M, Moritz C, Mable BK (Eds) Molecular Systematics. Sinauer Associates, Sunderland, MA, 205–247.

Paradis E, Claude J, Strimmer K (2004) APE: Analyses of phylogenetics and evolution in R language. Bioinformatics 20: 289–290. https://doi.org/10.1093/bioinformatics/btg412

Poe S, Nieto-Montes de Oca A, Torres-Carvajal O, de Queiroz K, Velasco JA, Truett B, Gray LN, Ryan MJ, Köhler G, Ayala-Varela F, Latella I (2017) A phylogenetic, biogeographic, and taxonomic study of all extant species of *Anolis* (Squamata; Iguanidae). Systematic Biology 66: 663–697. https://doi.org/10.1093/sysbio/syx029

Poe S, Scarpetta S, Schaad EW (2015) A new species of *Anolis* (Squamata: Iguanidae) from Panamá. Amphibian & Reptile Conservation 9: 1–13. https://doi.org/10.5281/zenodo.11148375

Pons O, Petit R (1996) Measuring and testing genetic differentiation with ordered versus unordered alleles. Genetics 144: 1237–1245. https://doi.org/10.1093/genetics/144.3.1237

Prates I, D'Angiolella AB, Rodrigues MT, Melo-Sampaio PR, de Queiroz K, Bell RC (2021) Evolutionary drivers of sexual signal variation in Amazon slender anoles. Evolution 75: 1361–1376. https://doi.org/10.1111/evo.14230

R Core Team (2025) R: A language and environment for statistical computing. R Foundation for Statistical Computing, Vienna. https://www.R-project.org

Rambaut A, Drummond AJ, Xie D, Baele G, Suchard MA (2018) Posterior summarization in Bayesian phylogenetics using Tracer 1.7. Systematic Biology 67: 901–904. https://doi.org/10.1093/sysbio/syy032

Revell LJ, Harmon LJ, Collar DC (2008) Phylogenetic signal, evolutionary process, and rate. Systematic Biology 57: 591–601. https://doi.org/10.1080/10635150802302427

Rivera-Correa M, Correa-Medina H, Venegas-Valencia K, Daza JM (2022) Genetic diversity, acoustic signal and geographic distribution of a colourful rain frog of the genus *Pristimantis* (Anura: Craugastoridae): Genetic diversity of the *Pristimantis jaguensis*. Herpetology Notes 15: 215–227. https://www.biotaxa.org/hn/article/view/70030

Rojas-Morales JA, Arias-Monsalve HF, González-Durán GA (2014) Anfibios y reptiles de la región centro-sur del departamento de Caldas, Colombia. Biota Colombiana 15: 73–93.

Ronquist F, Teslenko M, van der Mark P, Ayres DL, Darling A, Höhna S, Larget B, Liu L, Suchard MA, Huelsenbeck JP (2012) MrBayes 3.2: Efficient Bayesian phylogenetic inference and model choice across a large model space. Systematic Biology 61: 539–542. https://doi.org/10.1093/sysbio/sys029

Ruiz-García M, Arias-Vásquez JY, Restrepo H, Cáceres-Martínez CH, Shostell JM (2020) The genetic structure of the spectacled bear (*Tremarctos ornatus*; Ursidae, Carnivora) in Colombia by means of mitochondrial and microsatellite markers. Journal of Mammalogy 101: 1072–1090. https://doi.org/10.1093/jmammal/gyaa082

Santos JC, Coloma LA, Cannatella DC (2003) Multiple, recurring origins of aposematism and diet specialization in poison frogs. Proceedings of the National Academy of Sciences of the USA 100: 12792–12797. https://doi.org/10.1073/pnas.2133521100

Schneider CA, Rasband WS, Eliceiri KW (2012) NIH Image to ImageJ: 25 years of image analysis. Nature Methods 9: 671–675. https://doi.org/10.1038/nmeth.2089

Stapley J, Wordley C, Slate J (2011) No evidence of genetic differentiation between anoles with different dewlap color patterns. Journal of Heredity 102: 118–124. https://doi.org/10.1093/jhered/esq104

Tollis M, Ausubel G, Ghimire D, Boissinot S (2012) Multi-locus phylogeographic and population genetic analysis of *Anolis carolinensis*: Historical demography of a genomic model species. PLoS One 7: e38474. https://doi.org/10.1371/journal.pone.0038474

Townsend JH, Hofmann EP (2017) Origins and biogeography of the Anolis crassulus subgroup (Squamata: Dactyloidae) in the highlands of nuclear Central America. BMC Evolutionary Biology 17: 267. https://doi.org/10.1186/s12862-017-1115-8

Turner P, Corander J (2021) Boosting heritability: Estimating the genetic component of phenotypic variation with multiple sample splitting. BMC Bioinformatics 22: 1–16. https://doi.org/10.1186/s12859-021-04079-7

Wickham H (2016) ggplot2: Elegant Graphics for Data Analysis. Springer, New York, 260 pp.

Wickham H, François R, Henry L, Müller K (2021) dplyr: A Grammar of Data Manipulation. R package version 1.0.7.

Williams EE (1976) South American anoles: The species groups. Papéis Avulsos de Zoologia 29: 1–28. https://doi.org/10.11606/0031-1049.1976.29.p259-268

Wood ZT, Wiegardt AK, Barton KL, Clark JD, Homola JJ, Olsen BJ, King BJ, Kovach AI, Kinnison MT (2021) Meta-analysis: Congruence of genomic and phenotypic differentiation across diverse natural study systems. Evolutionary Applications 14: 2189–2205. https://doi.org/10.1111/eva.13264

Wüster W (2025) Shedding the mitochondrial blinkers: A long-overdue challenge for species delimitation in herpetology. Vertebrate Zoology 75: 259–275. https://doi.org/10.3897/vz.75.e161536

Zaher H, Prudente ALC (2003) Hemipenis of *Siphlophis* (Serpentes, Xenodontinae) and techniques of hemipenial preparation in snakes: A response to Dowling. Herpetological Review 34: 302–306.

Supplementary Material 1

Figures S1–S12

Authors: Grisales-Martínez FA, Daza JM (2026)
Data type: .pdf
Explanation notes: Figure S1. Variation in hemipenial morphology. **A**, **B**: Hemipenial type A (MHUA-R 15672 and 15771 respectively); **C**, **D**: Hemipenial type B (MHUA-R 15684 and 15788 respectively). — **Figure S2. A**) Allometric analyses show variation in head width (HW) and **B**) snout–vent length (SVL) between hemipenial morphotypes. — **Figure S3.** Variation in dewlap colour pattern. **A**, **B**, **C**: orange-yellow dewlap (MHUA-R 15650, 15671 and 15669 respectively); **D**, **E**, **F**: orange-pink dewlap (MHUA-R 15782, 15652 and 15773 respectively), **G**, **H**, **I**: reddish dewlap (MHUA-R 15674, 15673 and 15646 respectively). — **Figure S4.** DAPC scatterplot of dewlap variation. Individuals are distributed along the first two discriminant functions; dots represent individuals and colour indicate dewlap colour patterns. — **Figure S5.** Delta test for phylogenetic signal in traits. **A**) Hemipenial morphology and **B**) dewlap colour pattern. The light blue area represents the null distribution generated from 100 randomizations of trait states across the tree to assess statistical significance. — **Figure S6.** TCS network colored by hemipenial morphs based on 814 bp of 16S. — **Figure S7.** TCS network colored by dewlap colour pattern based on 814 bp of 16S. — **Figure S8.** TCS network colored by clades based on 814 bp of 16S. — **Figure S9.** TCS network colored by hemipenial morphs based on 1068 bp of ND2. — **Figure S10.** TCS network colored by dewlap colour pattern based on 1068 bp of ND2. — **Figure S11.** TCS network colored by clades based on 1068 bp of ND2. — **Figure S12.** TCS network colored by clades based on 800 bp of cyt *b*.
Copyright notice: This dataset is made available under the Open Database License (http://opendatacommons.org/licenses/odbl/1.0). The Open Database License (ODbL) is a license agreement intended to allow users to freely share, modify, and use this dataset while maintaining this same freedom for others, provided that the original source and author(s) are credited.
Link: https://doi.org/10.3897/vz.76.e195284.suppl1

Supplementary Material 2

Tables S1–S4

Authors: Grisales-Martínez FA, Daza JM (2026)
Data type: .zip
Explanation notes: Table S1. Specimen data including voucher, political and geographic location, sex, mitochondrial sampling with GenBank accession numbers, assignment to mitochondrial clade, and phenotypic trait (dewlap and hemipenes) [.txt file]. — **Table S2.** Primers used for amplification of mitochondrial regions with PCR conditions [.txt file]. —**Table S3.** Population genetics indices between different clades of *A. mariarum* calculated from nucleotide sequence of mitochondrial 16S, cyt *b* and ND2 regions [.txt file]. — **Table S4.** Mean uncorrected genetic distance matrix between mitochondrial clades of *A. mariarum* for the 16S, ND2, and cyt *b* mitochondrial markers [.txt file].
Copyright notice: This dataset is made available under the Open Database License (http://opendatacommons.org/licenses/odbl/1.0). The Open Database License (ODbL) is a license agreement intended to allow users to freely share, modify, and use this dataset while maintaining this same freedom for others, provided that the original source and author(s) are credited.
Link: https://doi.org/10.3897/vz.76.e195284.suppl2

Supplementary Material 3

Files S1–S14

Authors: Grisales-Martínez FA, Daza JM (2026)
Data type: .zip
Explanation notes: File S1. Assembled genetic dataset including mitochondrial regions 16S, ND2, cyt *b* [nexus file]. — **File S2.** Partitions and evolutionary models used in the phylogenetic analysis [nexus file]. — **File S3.** Genetic matrix for mapping dewlap colour variation onto a haplotype network for the 16S gene [nexus file]. — **File S4.** Genetic matrix for mapping hemipenial morphology variation onto a haplotype network for the 16S gene [nexus file]. — **File S5.** Genetic matrix for mapping mitochondrial clades onto a haplotype network for the 16S gene [nexus file]. — **File S6.** Genetic matrix for mapping dewlap colour variation onto a haplotype network for the ND2 gene [nexus file]. — **File S7.** Genetic matrix for mapping hemipenial morphology variation onto a haplotype network for the ND2 gene [nexus file]. — **File S8.** Genetic matrix for mapping mitochondrial clades onto a haplotype network for the ND2 gene [nexus file]. — **File S9.** Genetic matrix mapping dewlap colour variation onto a haplotype network for the cyt *b* gene [nexus file]. — **File S10.** Genetic matrix mapping hemipenial morphology variation onto a haplotype network for the cyt *b* gene [nexus file]. — **File S11.** Genetic matrix for mapping mitochondrial clades onto a haplotype network for the cyt *b* gene [nexus file]. — **File S12.** Complete maximum-likelihood (ML) phylogenetic tree in pdf format, including 137 terminals representing *Anolis mariarum* and closely related species of the *Anolis fuscoauratus* group. The tree was inferred from an alignment of 2687 sites across three mitochondrial DNA regions (16S, cyt *b*, and ND2) [pdf file]. **File S13.** Complete maximum-likelihood (ML) phylogenetic tree in Newick format, including 137 terminals representing *Anolis mariarum* and closely related species of the *Anolis fuscoauratus* group. The tree was inferred from an alignment of 2687 sites across three mitochondrial DNA regions (16S, cyt *b*, and ND2) [newick tree file]. — **File S14.** Complete 50% majority-rule consensus tree from the Bayesian inference (BI) analysis, in NEXUS format, including 137 terminals representing *Anolis mariarum* and closely related species of the *A. fuscoauratus* group. The tree was inferred from an alignment of 2687 sites across three mitochondrial DNA regions (16S, cyt *b*, and ND2) [nexus tree file].
Copyright notice: This dataset is made available under the Open Database License (http://opendatacommons.org/licenses/odbl/1.0). The Open Database License (ODbL) is a license agreement intended to allow users to freely share, modify, and use this dataset while maintaining this same freedom for others, provided that the original source and author(s) are credited.
Link: https://doi.org/10.3897/vz.76.e195284.suppl1